MASTER COPY KEEP THIS COPY FOR REPRODUCTION PURPOSES

REPORT DOCUMENTATION PAGE

Form Approved
OMB No. 0704-0188

Public reporting burden for this collection of information is estimated to average 1 hour per response, including the time for reviewing instructions, searching existing data sources, gathering and maintaining the data needed, and completing and reviewing the collection of information. Send comments regarding this burden estimate or any other aspect of this collection of information, including suggestions for reducing this burden to Washington Headquarters Services, Directorate for information Operations and Reports, 1215 Jefferson Davis Highway, Suite 1204 Arlington, VA 22202-4302, and to the Office of Management and Budget, Paperwork Reduction Project (0704-0188), Washington, DC 20503.

1. AGENCY USE ONLY (Leave blank)	2. REPORT DATE	3. REPORT TYPE AND DATES COVERED
	August 1, 1996	Final Technical Report

4. TITLE AND SUBTITLE
High Gain, Low Noise and Broadband Raman and Brillouin Fiber-Optic Amplifiers, Channel Selectors and Switches

5. FUNDING NUMBERS
DAAL03-91-G-0301

6. AUTHOR(S)
Chung Yu

7. PERFORMING ORGANIZATION NAME(S) AND ADDRESS(ES)
North Carolina A & T State University,
Greensboro, NC 27411

8. PERFORMING ORGANIZATION REPORT NUMBER

9. SPONSORING / MONITORING AGENCY NAME(S) AND ADDRESS(ES)
U. S. Army Research Office
P. O. Box 12211
Research Triangle Park, NC 27709-2211

10. SPONSORING / MONITORING

19960801 181

11. SUPPLEMENTARY NOTES
The view, opinions and/or findings contained in this report are those of the author(s) and should not be construed as an official Department of the Army position, policy, or decision, unless so designated by other documentation.

12a. DISTRIBUTION / AVAILABILITY STATEMENT
Approved for public release; distribution unlimited.

12b. DISTRIBUTION CODE

13. ABSTRACT

Wavelength independent Raman (sRs) and Brillouin (sBs) scattering processes in singlemode fibers have been exhaustively investigated for optical amplification - key to channel selection and switching in optical communication. The low gain and high pump threshold of sRs and the high gain, low pump threshold, but extremely narrowband sBs prevented further consideration of these processes for possible optical device fabrication for communication. Fiber rings have been employed to attempt to further lower the sBs threshold for optical switching with some success. However, such a device suffers from excessively long switching time of over 52 ns. Much work remains to improve the performance of fiber ring devices.

Dependence of sBs gain and shift on the elastic properties of the fiber material and geometry, and its close correlation with the forward spontaneous but resonant Brillouin scattering, coined GAWBS, via numerous models and experimental verification, point to the possibility of employing both processes for sensing fiber and ambient parameters, such as fiber chemical composition, fiber core and diameter variations, fiber strain, fiber and ambient temperature, etc. The forward and backward sensing capability may render such a sensor fault tolerant. The noise level sensing of GAWBS using electronic heterodyne technique imparts robustness to such a device. Work is ongoing in the practical implementation of the device for structural health monitoring via bonding and embedding.

14. SUBJECT TERMS	15. NUMBER OF PAGES
Brillouin Active Fiber Sensor and Optical Switch	34
	16. PRICE CODE

17. SECURITY CLASSIFICATION OF REPORT	18. SECURITY CLASSIFICATION	19. SECURITY CLASSIFICATION OF ABSTRACT	20. LIMITATION OF ABSTRACT
UNCLASSIFIED	UNCLASSIFIED	UNCLASSIFIED	UL

DISCLAIMER NOTICE

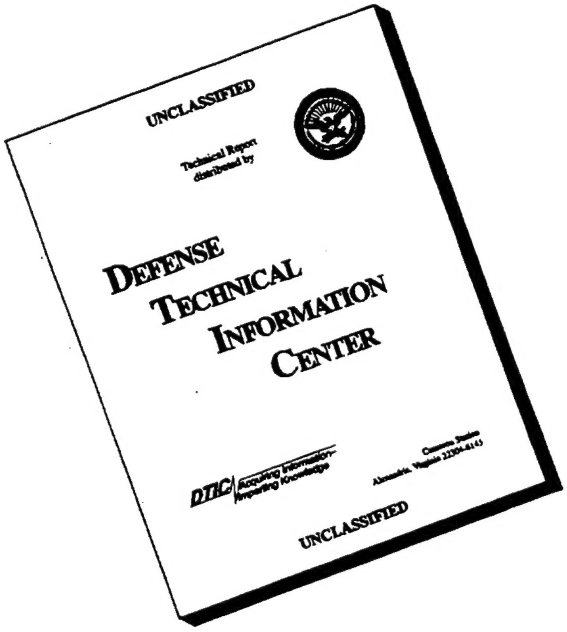

THIS DOCUMENT IS BEST QUALITY AVAILABLE. THE COPY FURNISHED TO DTIC CONTAINED A SIGNIFICANT NUMBER OF PAGES WHICH DO NOT REPRODUCE LEGIBLY.

HIGH GAIN, LOW NOISE AND BROADBAND RAMAN AND BRILLOUIN FIBER-OPTIC AMPLIFIERS, CHANNEL SELECTORS AND SWITCHES

FINAL REPORT

CHUNG YU

7/15/91 - 7/14/96

U.S. ARMY RESEARCH OFFICE

DAAL03-91-G-0301

ELECTRICAL ENGINEERING DEPARTMENT
NORTH CAROLINA A&T STATE UNIVERSITY
GREENSBORO, NC 27411

ABSTRACT

Wavelength independent Raman (sRs) and Brillouin (sBs) scattering processes in singlemode fibers have been exhaustively investigated for optical amplification - key to channel selection and switching in optical communication. The low gain and high pump threshold of sRs and the high gain, low pump threshold, but extremely narrowband sBs prevented further consideration of these processes for possible optical device fabrication for communication. Fiber rings have been employed to attempt to further lower the sBs threshold for optical switching with some success. However, such a device suffers from excessively long switching time of over 52 ns. Much work remains to improve the performance of fiber ring devices.

Dependence of sBs gain and shift on the elastic properties of the fiber material and geometry, and its close correlation with the forward spontaneous but resonant Brillouin scattering, coined GAWBS, via numerous models and experimental verification, point to the possibility of employing both processes for sensing fiber and ambient parameters, such as fiber chemical composition, fiber core and diameter variations, fiber strain, fiber and ambient temperature, etc. The forward and backward sensing capability may render such a sensor fault tolerant. The noise level sensing of GAWBS using electronic heterodyne technique imparts robustness to such a device. Work is ongoing in the practical implementation of the device for structural health monitoring via bonding and embedding.

TABLE OF CONTENTS

INTRODUCTION

ARO Grant DAAL03-91-G-0488 has received multi-year funding since 1991 with the initial objective of developing fiber based Raman and Brillouin active devices for optical amplification, channel selection and switching. The wavelength independent techniques of stimulated Raman and Brillouin scattering were investigated initially for feasibility of broadband Raman amplification, possibly enhanced by the stimulated Brillouin process to achieve high gain and low noise, while the high gain, low noise Brillouin fiber amplifier would be broadbanded using cascaded low-threshold fiber rings. These techniques have been studied at 10.6μm, and 1310nm wavelengths, with little success at the former due to lack of low-loss fibers and rather promising results at the latter wavelength with extremely low-loss singlemode fibers.

Most of the work has been focused on Brillouin active fiber based devices, since Raman fiber amplifier was long regarded as a poor substitute for the widely adopted erbium doped and praseodymium doped fiber amplifiers. We have made substantial progress in Brillouin active backward scattered 11 GHz Stokes line and the forward scattered Guided Acoustic Wave Brillouin Scattering (GAWBS) MHz spectrum, observed only in the confined geometry of a singlemode fiber. These phenomena are currently under intense study for possible application as fiber sensors for structural integrity.

The hitherto neglected Raman fiber amplifier will be re-examined since erbium doped and praseodymium doped fiber amplifiers perform lumped amplification, which lowers system reliability, and is further degraded by reliance on diode laser pumps and fragility and brittleness of fluoride based fibers. The Raman fiber amplifier, on the other hand, relies on the intrinsic amplification of the silica fiber with distributed gain increasing with effective fiber length. Its robustness is also derived from the use of multiple redundant laser diodes as driver. Further study is necessary on its amplification process, gain, linearity, distortion, cross talk and noise properties, and relationship to the Brillouin process.

The concept of stimulated Brillouin scattering (sBs) based optical switching using fiber rings has been explored theoretically and experimentally by us . So far, the questions have been switching speed as function of phonon lifetime, steady state gain and fiber ring buildup. The dependence of sBs on density fluctuations in low gain media places limitations on several switching factors such as pulse width, pulse repetition rate and threshold levels for logic "1" and "0". The pulsewidth to pulse period ratio also determines the maximum intensity required. The sBs logic gate has been shown to function as a true Fradkin gate, except for reversibility. Thus, higher order functions typical of most computers, such as the adder circuit, can be built using the sBs gate. The feasibility of using multiple fiber rings must also be investigated.

Table 1 Survey of Optical Fiber Amplifiers

Property	Praseodymium Fiber	Brillouin Fiber	Raman Fiber	Erbium Fiber
Unsaturated device gain	> 30 dB	20 dB	5 - 10 dB	> 20 dB
Optical pump power		< 10 mW	100 - 200 mW	20 - 50 mW
Optical pump wavelength	1047 nm	Stokes shift below signal λ		807 nm, 980 nm, 1460 - 1500 nm
Electrical bias current	N/A	< 50 mA	> 500 mA	> 100 mA
Wavelength of operation	1300 nm	Any, but subject to pump λ		1530 - 1560 nm
Stokes shift		0.1 nm	100 nm	N/A
Bandwidth	30 nm	0.001 nm	20 - 40 nm	10 - 40 nm
Coupling loss		< 1 dB	< 1 dB	< 1 dB
Polarization sensitivity		0 dB	0 dB	0 dB
Saturated output (-3 dB)	0.18 dBm or 65 mW	Limited only by pump power		few mW
Direction		Unidirectional	Bi-directional	Bi-directional
Noise	8 dB	Very low	Very low	Low
Cross-talk		N/A	Low	Only below 100 kHz
Intermodulation distortion		N/A	Low	Only below 100 kHz
Commercial Availability	Yes	N/A	No	Yes
Price	$35,000	N/A	Few $K	$50,000
Reliability	Poor (Britle Fluoride Fiber)	N/A	Potentially High	Moderate
Concurrent 1310, 1550 nm Operation	No	N/A	Yes	No
Switching	Poor	Yes (Good)	No	Poor

Gain/Bandwidth Comparison for Fiber Amplifiers

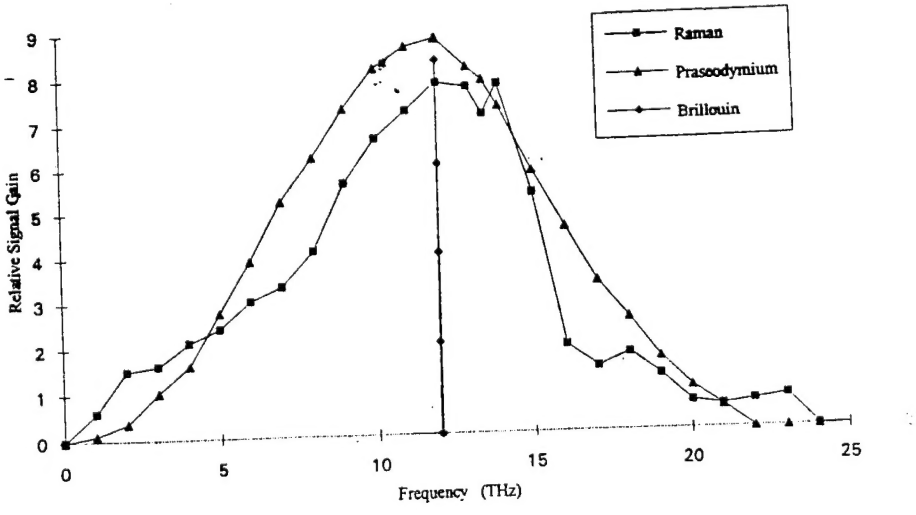

THE RAMAN FIBER AMPLIFIER FOR OPTICAL COMMUNICATION

The polarization-independent gain with minimum number of interfaces, large saturation output power, high speed response and broad bandwidth are attractive properties of the fiber Raman amplifier for WDM amplification. The Raman technology is superior to doped technologies -- erbium and praseodymium, since distributed amplification has advantages over lumped amplification. The use of several generations of Raman Stokes and anti-Stokes lines to achieve operation at both 1310 and 1550 nm wavelength is highly attractive. Such amplifiers can potentially reduce cost to 1/10 of that of a repeater, raise the signal-to-noise ratio and handle higher transmission speeds.

At present, both erbium and praseodymium doped fiber amplifier have system reliability problems, i.e., when they malfunction, the entire system is affected. Single or two-laser pump sources also render the system less robust. Praseodymium fiber amplifier also uses brittle and fragile fluoride-based fibers. Neodymium doped fiber is proposed as the pump source in the Raman fiber amplifier, but not the amplification medium, which is rugged silica fiber. Such an amplifier can be driven by multiple low cost laser diodes, with built-in heavy redundancy.

RESEARCH WORK ON FIBER RAMAN AMPLIFIER

As is evident from the Table, the fiber Raman amplifier has a very broad bandwidth, but required substantial pump power. Furthermore, when using Raman amplifier in long-haul coherent systems, various schemes for the suppression of sBs, which causes pump depletion, have to be used. However, it has been found that the sBs threshold decreases dramatically in the presence of linear gain, generated by the Raman process. The presence of sBs also increases noise in the system significantly. It is thus fundamental that the sBs process be explored for the possibility of its elimination together with noise or its utilization in the enhancement of the Raman amplification process.

THE BRILLOUIN FIBER AMPLIFIER FOR OPTICAL NOISE SENSING AND SWITCHING

Brillouin fiber amplifiers can provide gains using modest pump powers. However, the gain bandwidth product is inherently small (17 MHz at 1.5 μm) and the spontaneous noise is substantially higher than that observed with other optical amplifiers, leading to a 20 dB noise figure for a typical preamplifier application. Although the gain bandwidth may be increased to accommodate data rates up to a few Gbit/s, the spontaneous emission noise will inevitably degrade the system performance. The large noise figure and narrow bandwidth of the fiber Brillouin amplifier render it quite noncompetitive. However. its high gain for backward wave scattering and high noise content renders the process highly suitable for ambient sensing.

CH 2. SBS PHOTONIC SWITCHING

The characteristics of sBs that are important in optical switching and hence optical computing are: phonon lifetime, steady state gain, sBs threshold, and fiber ring buildup time.

The threshold power for sBs in a fiber

$$P_{th} = 2I\frac{A}{g_B L_e}$$

where g_B = gain coefficient, I = intensity of the incident beam, L_e = effective length of fiber given by $L_e = 1/\alpha[1 - e^{-\alpha L}]$, and L = length of fiber.

The threshold power for sBs in a fiber is

$$P_{th} = \frac{2A}{g_B L}\frac{\pi^2}{F^2}$$

where A is the cross sectional area of the core and F is the finesse of the ring resonator given as a function of the coupling constant, K_r, of the ring: $F = (\pi K_r^{1/2})/(1 - K_r)$
Brillouin gain coefficient,

$$g_B = \frac{2\pi n^7 P_{12}^2}{c\lambda^2 \rho v_S \Gamma_B}$$

where n is the index of refraction, P_{12} is the elastooptic coefficient of the material, c is the speed of light, λ is the wavelength of the laser, ρ is the density of the material, and Γ_B is the Brillouin linewidth.

Standard values for fused silica are follows: $\rho = 2.21x10_3$ kgm^{-3}, n = 1.45, $P_{12} = 0.286$, $v_s = 5.97x10^3$ m/s, $\Gamma_B = 23$ MHz

The photon linewidth is much narrower than the phonon linewidth so that the lifetime of the sBs process is determined by the latter.

The linewidth is a transition per unit time and is given by

$$\Gamma_B = \frac{\eta_s k_B^2}{\rho_0}$$

where η_s = viscosity, ρ_0 = density, and k_B = wave vector of the scattered wave. The switching time for stimulated Brillouin scattering is therefore the inverse of the linewidth which is the phonon lifetime. The phonon lifetime is given by

$$\tau_B = 1/\Gamma_B$$

When dealing with pulses as in optical switching and computing, stimulated Brillouin scattering's dependence on density fluctuations in small gain media places limitations on several switching factors including: pulse width, period of pulses, and threshold levels for logic "1" and logic "0".

The intensity of the Stokes pulse is determined to be

$$\frac{I_s}{I_s(0)} = 1 + gI_0z(1 - e^{-\tau})$$

where the higher order terms have been ignored.

The Stokes intensity at the end of the Nth pulse is given by

$$\frac{I_s}{I_s(0)} = 1 + gI_0z\left(\frac{\tau_p}{\Delta}\right)(1 - e^{-N\Delta})$$

where the pulse width and the period were taken to be very small.

Both the intensity of a single pulse and the intensity at the end of the Nth pulse were computer simulated. The pulse width was altered in order to determine the pulse width to period ratio suitable for proper switching by defining the intensity function, V, such that $V = 1 - e^{-\tau}$ for the continuous wave, and $V = \tau_p/\Delta(1 - e^{-N\Delta})$ for the pulses.

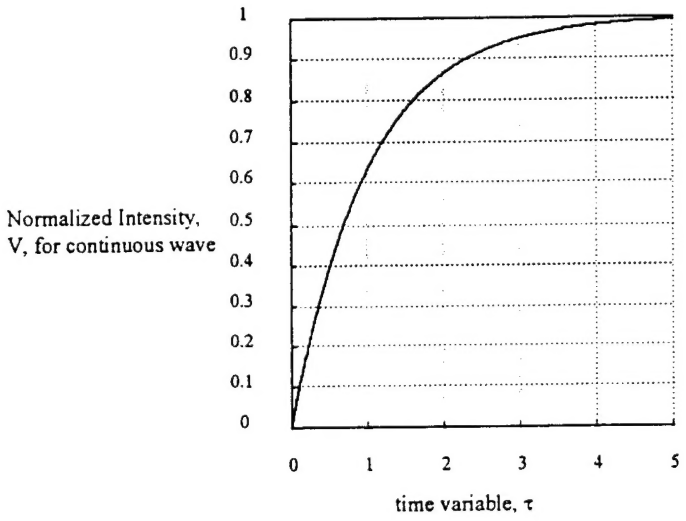

Graph of Normalized Output Intensity, V vs. time, τ

The time was normalized to twice the phonon lifetime so that normalized time constant is given by $\tau = t/2\tau_B$. It was observed that the intensity of the Stokes wave approximated the input laser intensity after 4 time constants.

The induced Stokes wave is the product of two incident laser beams. Therefore, a logic "1" will be detected when the normalized intensity becomes at least 0.5. Any normalized intensity that is lower than 0.5 was determined to be logic "0". The pulse width of 66 ns was extrapolated to be 75% of the time constant.

Investigation of the pulse widths and periods leads to conclusions for determining the minimum allowable pulse width and period ratio for this type of switching mechanism. The pulse width to period ratio also plays an important role in determining the maximum intensity of the system. Even though the intensity of the driving pulses are high, the resultant switched intensity will only approach the pulse width to period ratio as a steady state value. In fact, if the pulse width to period ratio is too small, a logic "1" may never be attained. The pulse width was altered to determine steady state ratio of the system when pulses are used. When the pulse width accounts for 50% or more of the period, then a logic "1" could be produced.

As the pulse width to period ratio increased, the steady state gain of the continuous wave was approximated. When the continuous wave normalized intensity approaches unity, the output Stokes wave intensity approximates the input laser intensity. The stokes wave will have enough intensity to stimulate another scattering process if other switches are cascaded, the pulse width and period ratio must be adjusted so that the intensity ratio must between 50% - 75%. If an average value (62.5%) is assumed for the pulse width to period ratio, then the delay time between pulses is determined to be approximately 39.6 ns.

Another static hazard is detected if one considers the fiber ring and the pulse widths. The fiber ring loop must be long enough to hold a pulse to the following reasons. Firstly, if the ring is too small, light from port #1 will destructively interfere with the light from port #2 as it emerges to port #4; this in effect may destroy potential data. Secondly, if the ring size is too large and more than one pulse traverses the ring, any pulse following too closely to a pulse that is backscattered by sBs phenomenon may be erroneously backscattered. The second condition places a limitation of the minimum delay of the system; the delay is adjusted so that the density fluctuations in the medium do not scatter a secondary pulse in error.

An optical module that uses the switching property of sBs in a fiber ring may be created, but there are limitations accompanying the switching phenomenon and the ring. Any system utilizing the switching property of pulsed sBs in a fiber ring is constrained. Limitations were noted in the pulse width, where pulse widths could not be too small or too large. It was noted that the pulse width had to account fir at least 50% of the period. The delay times between pulses were also observed to be an appreciable factor.

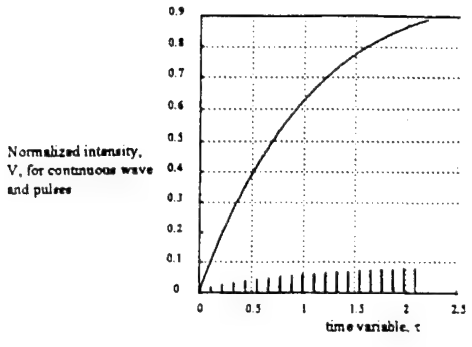

t_p=.01, t_d=.1, t_p / Δ =.091

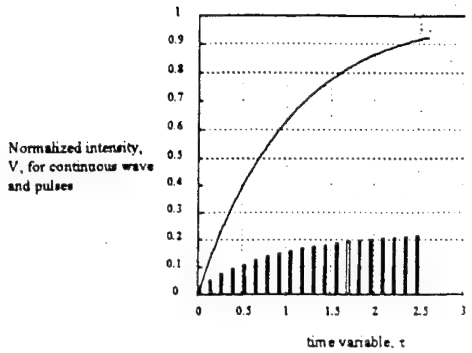

t_p=.03, t_d=.1, t_p / Δ =.23

Graph of pulsed normalized intensities where pulse widths are 9.1% and 23% of the period

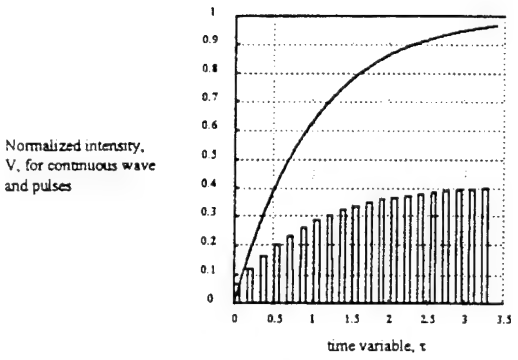

t_p=.07, t_d=.1, t_p/Δ =.41

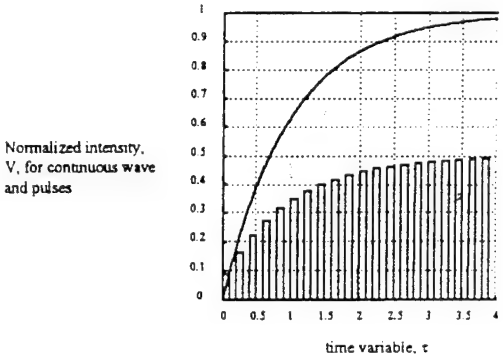

t_p=.1, t_d=.1, t_p/Δ =.5

Graph of pulsed normalized intensities where pulse widths are 41% and 50% of the period

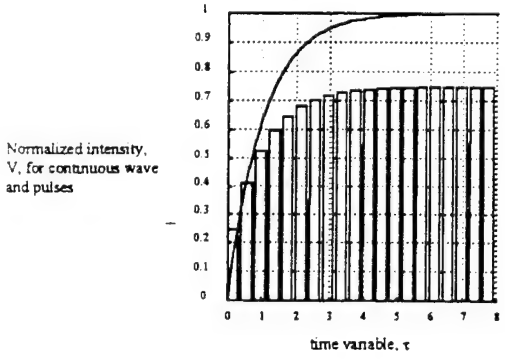

t_p = .3, t_d=.1, t_p/Δ = .75

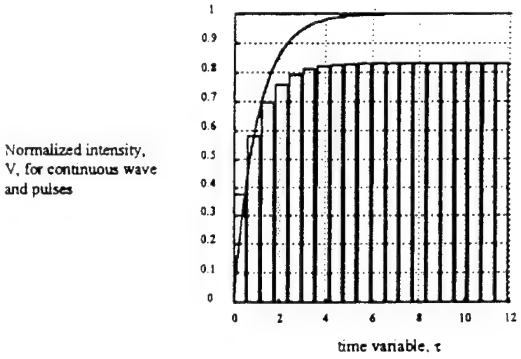

t_p = .5, t_d=.1, t_p/Δ = .83

Graph of pulsed normalized intensities where pulse widths are 75% and 83% of the period

SBS BASED OPTICAL SWITCHING USING A FIBER RING

The pump power levels required for sBs generation is greatly reduced in high-finesse, singlemode all fiber-ring resonators, with reported thresholds as low as 70 μw. Submilliwatt Brillouin thresholds and linewidth narrowing have been demonstrated in an all-fiber resonator using AlGaAs laser diodes as pump source. By pumping the ring laser below threshold, it can act as an effective amplifier of signals at the Stokes frequency.

High gain is predicted for such an amplifier with resonator of short loop length, requiring very low pump powers (<0.1 μw). Corresponding output SNR is very highg (>55 dB) even for very small signals, and improves with increasing signal level and loop length.

For a ring of length 1m and finesse of 260, the number of rotations needed before the threshold is reached may be extrapolated graphically. The number of rotations was determined to be approximately 1 in order to reach the threshold power of 5 mw for 1.3 μm wavelength; assuming the total incident power into the ring was 5 mW.

The total switching time of the fiber ring is given by the following:

$$t_{Total} = \tau_B + t_{power\ buildup} + t_{exit\ from\ ring}$$

where $t_{Power\ buildup}$ = time to build up sBs threshold power; $t_{exit\ from\ ring}$ is the time taken for the Stokes wave to exit from the ring. If the speed of light in monomode fiber is approximately $2.3x10^8$ m/s, then the total time is calculated from the velocity of the light in the fiber and distance that the light travels. The phonon lifetime value was determined from parameters taken from Cotter using a 1 m fiber.

$$t_{Power\ buildup} = 1m \times \frac{1}{2.3x10^8\ m/s} \approx 4.35ns \quad t_{Exit\ from\ ring} = 1m \times \frac{1}{2.3x10^8\ m/s} \approx 4.35ns$$

$$\tau_B = \frac{1}{23 \times 10^8\ 1/s} \approx 43.48ns$$

Therefore, the total amount of time to switch light using sBs in a fiber ring is 52.18 ns. The phonon lifetime accounts for slightly more than 80% of the total switching time. It is also noted that phonon lifetime is dependent on the media, different ring size and threshold power; however, the buildup time and exit time are not major parameters affecting switching time.

When the conttinuous wave normalized intensity approaches unity, the output Stokes wave intensity approximates the input laser intensity. The Stokes wave will have enough intensity to sttimulate another scattering process if other switches are causing logic hazard. Another static hazard is detected if one considers the fiber ring and the pulse widths. The fiber ring loop must be long enough to hold a pulse.

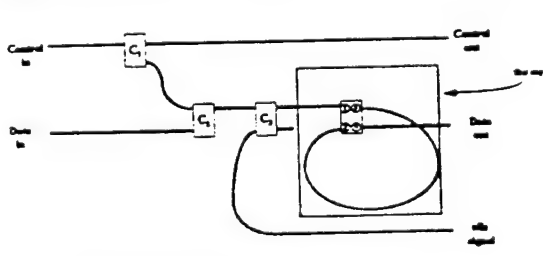

Internal structure of the sBs logic gate

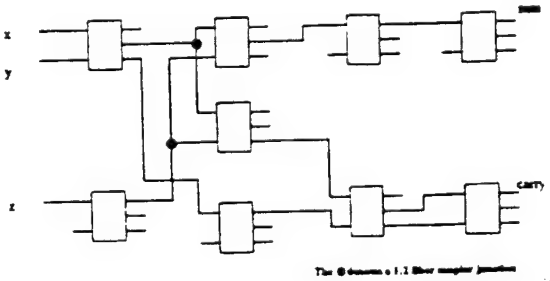

EXPERIMENTAL RESULTS ON SBS SWITCHING

The photodetector output was also taken at varied input intensities and is shown in Fig.

The ramp waveform represents piezo control signal sweep. The pulse train riding on the ramp signal is interpreted to be the onset of sBs at each ring resonance. We held the frequency at a constant value of 40 Hz, while observing changes in the number, and the shape of the peaks by varying the input intensity.

Lowering the frequency of the ramp control signal while holding the power constant caused instability in the output signals recorded by both detectors. When adjusted near the highest piezo frequency, sBs signal also became unstable, indicating higher sBs threshold. Adjusting the amplitude of the ramp signal driving the piezo, while holding the frequency and power constant, caused instability, due possibly to insufficient sBs evolution time.

The PZT driven fiber ring cannot perform as an effective optical switch because the cyclic resonance of the device does not allow stable switching states. Once the sBs phenomenon begins to evolve, it is interrupted when the ring goes off resonance. A virtually static resonant fiber ring is essential for optical switching using sBs. Once such a ring is established, then the theoretically predicted switching performance can be tested and implemented. Such a fiber ring switch can then be optimized as regards to fiber length, fiber index of refraction, coupler efficiency, etc. It is also suggested that in future experiments of this type, the fiber length be varied for possible lower sBs, as well as the usage of different fiber types.

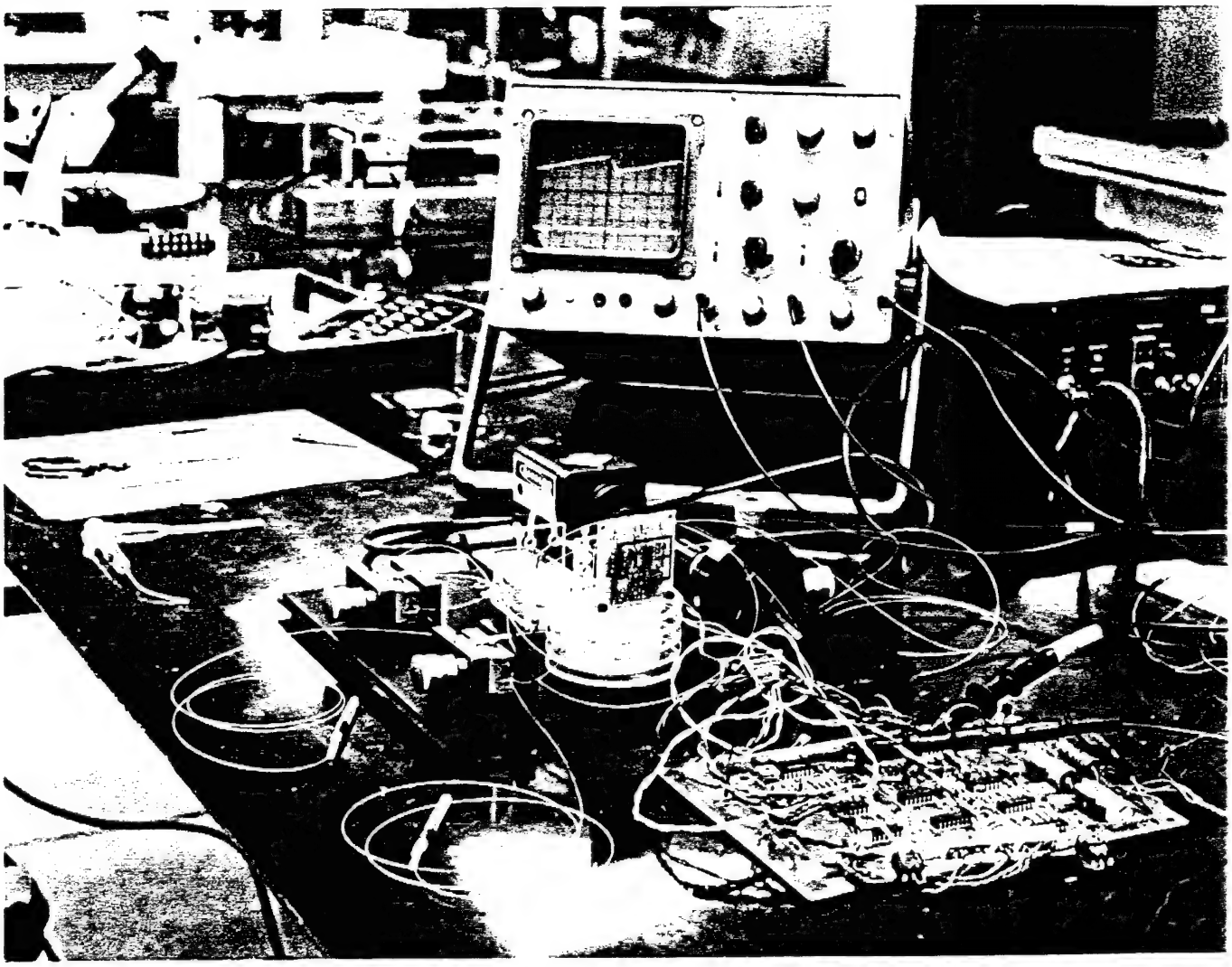

Fiber Ring

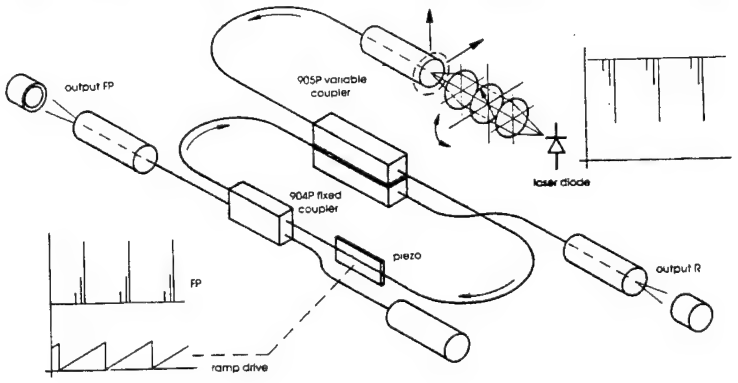

Schematic

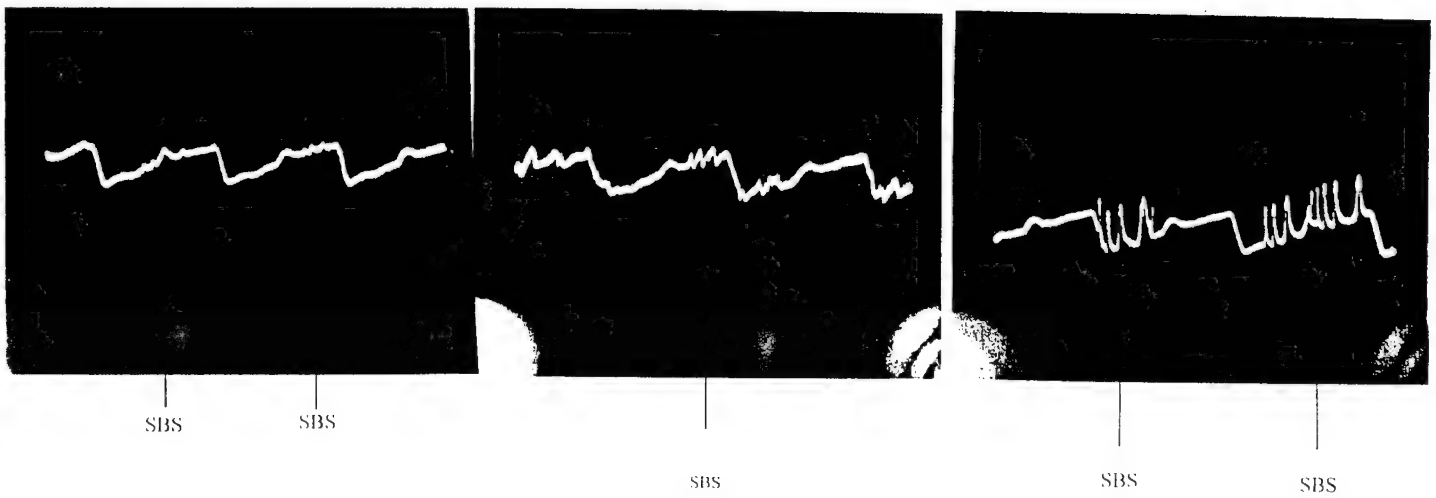

Real-Time SBS Occurrence at Minimum Power

Real-Time SBS Occurrence at Half Power

Real-Time SBS Occurrence at Maximum Power

CH 3. BRILLOUIN ACTIVE OPTICAL FIBER SENSING

A low loss silica fiber can readily exhibit Brillouin activity in both stimulated Brillouin scattering (sBs) and near-resonant forward (and backward) guided acoustic wave Brillouin scattering (GAWBS) with both polarized and depolarized components. The former is caused by longitudinal and the latter by longitudinal and torsional-radial phonons of the fiber.

Recently, fiber based sBs active sensors for temperature and strain have been reported while fiber based GAWBS active sensor has not been extensively studied. A status review on sBs sensors is given in Table 2. Since sBs theory is well established, only experimental schemes and data are highlighted in the table.

Table 2: Available SBS Experimental Data As Sensing Mechanism

Reference	SBS	Experimental Setup
Bao (1994)	Purpose: For distributed temperature and strain sensor based on Brillouin loss 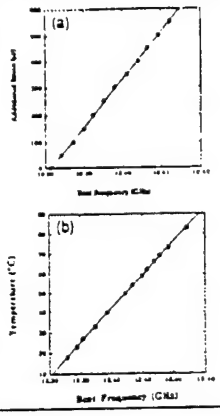	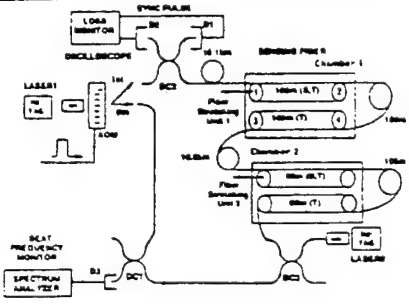 Parameter: - Laser: Both lasers were solid-state cw diode pumped Nd:YAG ring lasers emitting close to 1319nm. - Max. Power: ≈10mW - Fiber length: 22km

We have studied GAWBS extensively and have always observed the phenomenon at much lower incident laser powers and shorter fiber lengths as compared to the observation of sBs. This immediately connotes the potential superiority of the GAWBS sensor. To explore this fact in depth, the status of the GAWBS theory is revisited with additional confirmation from various viewpoints. A number of concepts are presented in Table 3.

This forward scattering mechanism has apparently been theorized and observed by a number of researchers. Their apparent divergent views are actually consistent when assembled, compared and properly interpreted. For instance, Stone attributed line broadening by Rayleigh-Brillouin scattering, to diffraction by a finite aperture, which is the radius of the fiber. Based on fiber parameters and laser wavelength, he arrived at a maximum broadening of 500 MHz. Jen analyzed this phenomenon as acousto-optic interaction, arriving at the conclusion that only R_{0m}, R_{2m}, L_{0m}, L_{2m}, TR_{2m}, respectively radial (R), longitudinal (L) and torsional-radial acoustic modes are allowed. This is consistent with Shelby's and Marcuse's findings. Marcuse predicted depolarization of incident laser light in the fiber due to birefringence caused by periodic variations in the fiber diameter. Shelby derived formulas for the experimentally observed fiber acoustic eigenmodes with specific mode frequencies, which have been confirmed by Shiraki, us and others (see Table 4). The depolarizing TR_{2m} modes have been simulated graphically, showing the greatest amount of depolarizing scattering when the center of the fiber core becomes strongly elliptical (see below). Shelby also predicted extremely low TR mode scattering efficiency, leading us to call such low level scattering "noise". However, this readily observed "noise" over the strongly coherent sBs frequency shift is aptly explained by Corvo, who carried out an extensive spatial-temporal Fourier analysis of forward Brillouin scattering. He concluded theoretically that GAWBS would dominate over sBs for long pulse or cw lasers, and also correctly predicted the frequency shift increase with increasing diffraction angle, as observed by us.

Table 3 SBS AND GAWBS MODELING

References	Bragg Condition $f_B=(f_B)_\pi \sin\frac{\theta}{2}$	
	sBs ($\theta=\pi\pm\delta\theta$)	GAWBS ($\theta=0^\circ\pm\delta\theta$)
Stone J. (1983)	Fused quartz: $(f_B)_\pi$=12.6GHz at λ=1.3μm, $\delta\theta=\lambda/\pi na \approx 0.08$	
	Linewidth: $\delta f_B=\frac{1}{4}(f_B)_\pi(\delta\theta)^2$<<100MHz	Linewidth: $\delta f_B=\frac{1}{2}(f_B)_\pi \delta\theta \cong 500$MHz
Jen C.K. (1989)	$\frac{dA_i(z)}{dz}=-jC^*(z)A_d(z)$ $-\frac{dA_d(z)}{dz}=-jC(z)A_i(z)$ where A_i and A_d are amplitudes of incident and diffracted optical waves, respectively. $C=C^r+C^z+C^{r\phi}+C^{\phi z}$ $C^{r\phi}, C^{\phi z} \ll C^r, C^z, C^{rz} \cong 5\% C^r$ C^r for L_{01}=sBs dominates (L_{0m}, L_{2m})	$C^r=b\iint(E_r^*\Delta\varepsilon_{rr}E_r+E_\phi^*\Delta\varepsilon_{\phi\phi}E_\phi)rdrd\phi$ $C^z=b\iint E_z^*\Delta\varepsilon_{zz}E_z rdrd\phi$ $C^{rz}=b\iint E_r^*\Delta\varepsilon_{rz}E_z rdrd\phi$ $C^{r\phi}=b\iint E_r^*\Delta\varepsilon_{r\phi}E_\phi rdrd\phi$ $C^{\phi z}=b\iint E_\phi^*\Delta\varepsilon_{\phi z}E_z rdrd\phi$ where $b=\omega_o\varepsilon_o/4$ $\Delta\varepsilon_{rr}=q[p_{11}(r)S_{rr}+p_{12}(r)S_{\phi\phi}+p_{12}(r)S_{zz}]$ $\Delta\varepsilon_{\phi\phi}=q[p_{12}(r)S_{rr}+p_{11}(r)S_{\phi\phi}+p_{12}(r)S_{zz}]$ $\Delta\varepsilon_{zz}=q[p_{12}(r)S_{rr}+p_{12}(r)S_{\phi\phi}+p_{11}(r)S_{zz}]$ $\Delta\varepsilon_{rz}=2qp_{44}S_{rz}$ $\Delta\varepsilon_{r\phi}=2qp_{44}S_{r\phi}$ $\Delta\varepsilon_{\phi z}=2qp_{44}S_{\phi z}$ where $q=-n^4(r)$ $S_{rr}, S_{\phi\phi}, S_{zz} \propto \cos n\phi$ $\quad S_{\phi r}, S_{\phi z} \propto \sin n\phi$ for HE_{11}: $E_r \propto \cos\phi$, $E_\phi \propto \sin\phi$, $E_z \propto \cos\phi$ $\therefore c=0$, except for $n=0, 2$ only F_{2m}, + R_{0m}, $= TR_{2m}$
Marcuse D. (1991)	Predicted depolarization of incident laser light in the fiber by periodic variation in the fiber diameter causing birefringence in the fiber.	$r=a_o+f\sin 2\phi$ $K_{00}=-i\frac{fK^2\gamma^2}{4n_1a_o k\beta^2}F$ $\quad F=1+\left(1-\frac{\gamma^2}{K^2}\right)\frac{J_o^2(Ka_o)}{J_1^2(Ka_o)}+\frac{(\gamma a_o)^2J_o^3(Ka_o)}{Ka_oJ_1^3(Ka_o)}$ $\frac{f\Delta^{3/2}}{a_o^2}L_p=\frac{\pi V^3}{\sqrt{2}(Ka)^2(\gamma a)^2F}=2.5$ L_p is the length required for the polarization to rotate by 90° a_o=5μm , Δ=0.00137, V=2.4 For f=0.05μm (1% elliptically), L_p=25m
Corvo A. (1988)	Concluded theoretically that GAWBS would dominate over sBs for long pulse or cw lasers, and also correctly predicted the frequency shift increase with increasing diffraction angle.	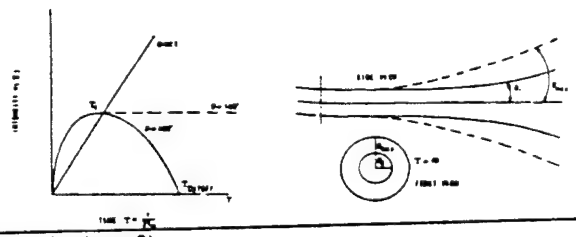
Shelby R.M. (1985)	First group to predict GAWBS.	TR_{2m} modes ($q_{//} \approx 0$) Light propagating with linear polarization at ϕ=45° encounter anisotropic perturbations which cause unequal phase shifts for components projected on the ϕ=0° and ϕ=90° axes. Polarization components are created along ϕ=±45° that are frequency up shifted and down shifted by the vibrational mode. The fraction depolarized in this way by the index perturbations is $\eta_f\frac{n^6\omega^2kT(A_1-\alpha^2A_2)^2(P_{11}-P_{12})^2}{64\pi c^2\rho V_s^2\alpha^2B_{T_m}} \approx 10^{-12}$ cm^{-1} for TR_{2s} mode The frequency shift f_m of the light wave scattered due to TR_{2m} modes is expressed as $f_m=\frac{V_s y_m}{\pi d}$ where V_s denotes the sound velocity of the shear wave and d is the fiber diameter. y_m is the eigenvalue related to the frequency f_m of the light scattered by TR_{2m} mode and is obtained by solving the following equation, which is determined by boundary conditions for TR_{2m} modes corresponding to zero traction on the fiber surface, $\begin{vmatrix}\left(3-\frac{y_m^2}{2}\right)J_2(\alpha y_m) & \left(6-\frac{y_m^2}{2}\right)J_2(y_m)-3y_mJ_3(y_m)\\ J_2(\alpha y_m)-\alpha y_mJ_3(\alpha y_m) & \left(2-\frac{y_m^2}{2}\right)J_2(y_m)+y_mJ_3(y_m)\end{vmatrix}=0$

Table 4 Available GAWBS experimental data

Reference	GAWBS	Experimental Setup
(a)Shelby R.M. (1985)	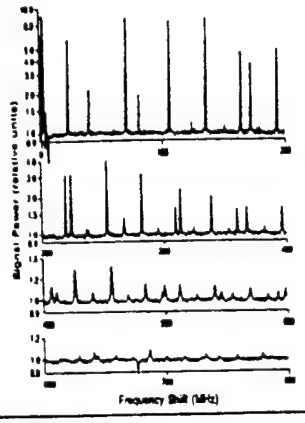	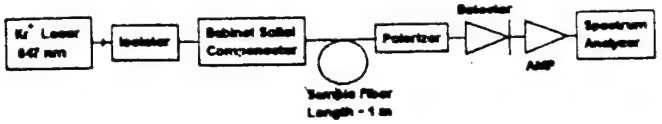 Parameters: - Laser: 647nm Kr^+ Spectra-Physics laser - Fiber Length: 1m singlemode fiber - Core: 4±0.4μm germania-doped silica - Cladding: 125±3μm pure synthetic silica - Input power: 200mW - Output power: 1-5mW - Pump linewidth: few MHz
(b) Poustie (1992)	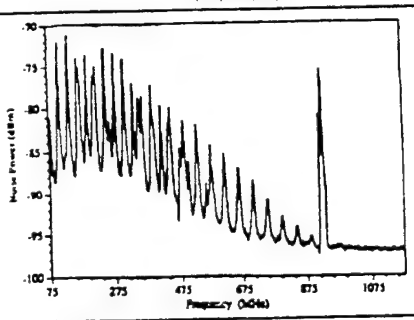	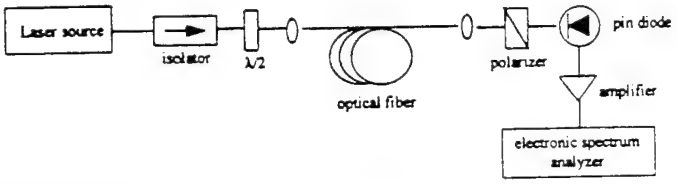 Parameters: - Laser: 1321nm 50 mW CW multimode Nd:YLF laser - Fiber length: 4000m standard telecommunication fiber
(c) Perlmutter (1990)	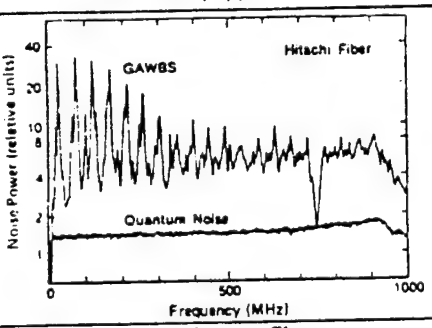	Parameters: - Fiber length: 100 m - Fiber type : Single-mode fused-silica optical fiber - Fiber core: ~ 5 μm - Fiber cladding: ~ 125 μm
(d) Yu (1994)	GAWBS spectrum for test fiber 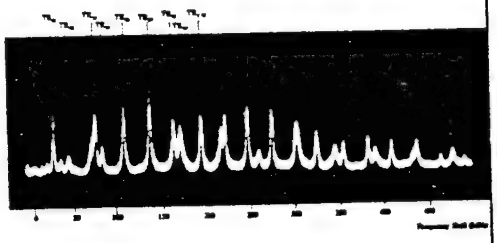	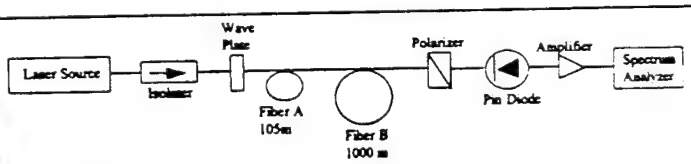 Parameters: - Laser: 1319nm Nd:YAG ring laser - Laser linewidth: < 10kHz - Fiber type : "Z" fiber from *LITESPEC Inc* - Fiber length: 1000 m
(e) Shiraki K. (1992)	GAWBS spectrum 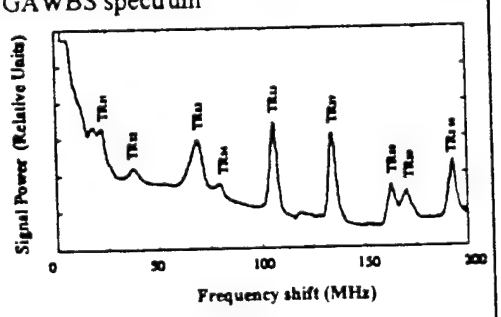	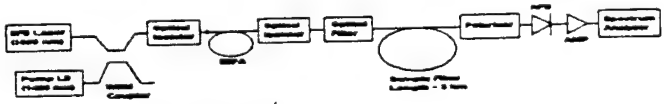 Parameters: - Laser: 1550nm DFB laser - Fiber length: 3000m - Core: 5μm pure silica - Cladding: 126±0.3μm (F-doped silica) - Input power: 2mW - Pump linewidth: <200 kHz

Table 5. SBS and GAWBS Corrleation

Types of scattering	Stimulated Backward Brillouin scattering	Stimulated Forward Brillouin scattering	Spontaneous Forward Brillouin scattering	Spontaneous Backward Brillouin scattering
	$f_a = \frac{2nV_a}{\lambda_p}\sin\frac{\theta}{2}$		$\delta f_B = \frac{1}{2}(f_B)_\pi \delta\theta$	$\delta f_B = \frac{1}{4}(f_B)_\pi (\delta\theta)^2$
Define θ 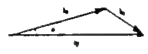	$\theta = 180^\circ$	$\theta = 0^\circ$		
Phonon Involved	Longitudinal $q_{//} \neq 0$, $q_\perp = 0$	—	Transverse $q_{//} = 0$, $q_\perp \neq 0$	Transverse $q_{//} = 0$, $q_\perp \neq 0$
Physical Mechanism	k-diagram 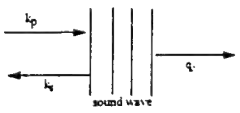	Cannot Construct	k-diagram 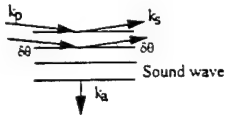	Cannot Construct
ω-k diagram	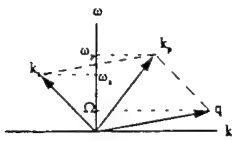	Cannot Construct	$q_{//}=0$ does not exist	$q_{//}=0$ does not exist
Conclusion	Possible	Not Possible	Possible	Not Possible

Table 6. Diffraction Model Experimental Verification

Reference	Pump Wavelength (λ)	Core radius (a)	δθ=λ/πna and n=1.46	$(f_B)_\pi$ GHz	Observed $(\delta f_B)_\pi$ MHz	Calculated Forward GAWBS $(\delta f_B)_\pi = (f_B)_\pi \times \delta\theta/2$ MHz
Stone	1.3 μm	3.5 μm	0.08	12.7	—	508
Shelby	0.647 μm	2.0 μm	0.0686	26.5	800	910
Shiraki	1.55 μm	2.5 μm	0.135	11.3	—	764
Yu	1.319 μm	3.19μm	0.0901	13.2	550	595
		3.47μm	0.0829		600	547
		4.59μm	0.0626		400	413
		4.9 μm	0.0587		400	387
Poustie	1.064 μm	1.5 μm	0.155	16.4	1200	1271
		2.0 μm	0.116		850	952
		3.0 μm	0.077		600	632

Table 7. Comparison of Sensing Capabilities of sBs and GAWBS

	SBS	GAWBS	
		Expected	Observed
Shift due to chemical composition	✓	✓	✓
Shift due to temperature	✓		
Shift due to stress	✓		
Shift due to fiber core size		✓	✓
Shift due to fiber cladding size		✓	✓
Linewidth due to coating		✓	✓

SBS AND GAWBS GENERATED ACOUSTIC WAVES IN FIBER

It is well known that Brillouin gain and frequency shift are dependent on the elastic properties of fiber materials, such as sound velocities, density, Young's modulus, etc. Therefore, the stimulated Brillouin frequency changes with fiber material and dopant concentration. The dopant dependence of sound velocity of longitudinal acoustic wave has been observed in backward or stimulated Brillouin scattering. These longitudinal sound waves in the fiber are also termed dilational waves, and they form a family of waves distinct from radial, torsional and mixed radial/torsional waves.

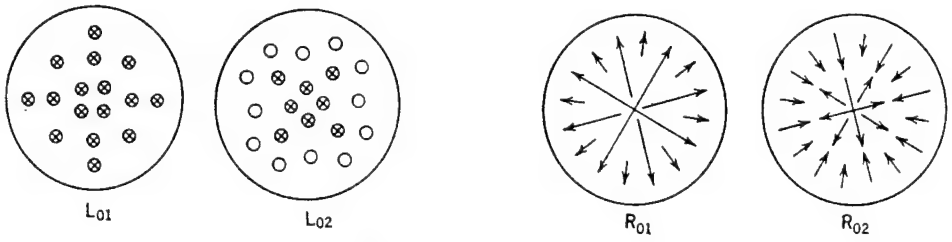

Schematic particle displacement patterns for the lowest order dilatational modes of a circular rod at $\beta = 0$.

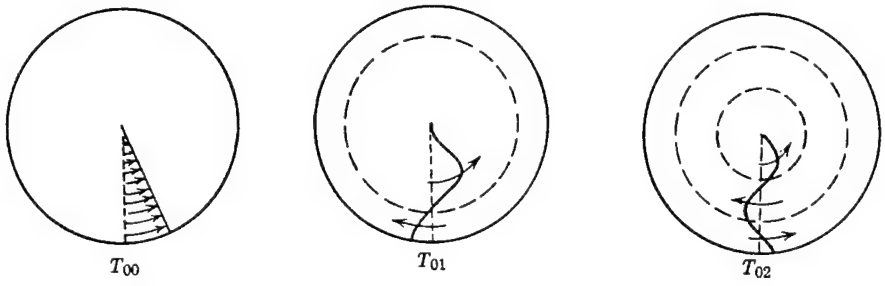

Particle velocity distributions for the three lowest order members of the torsional mode family T_{0q}.

The longitudinal or dilational modes possess particle velocity fields that have a radial component, which does not vary azimuthally, so that the free boundary alternately dilates and contracts. Thus, these modes can be subclassified according to their axial and radial motions at $\beta = 0$, and designated as L_{0q} and R_{0q} modes. In torsional modes, the particle velocity is entirely azimuthal. It vanishes at r = 0 and alternates in sign with increasing r. The designation T_{0q} . For this type of modes, each cross section of the rod (fiber) rotates rigidly about the axis. Propagation is at the bulk shear velocity V_s - $(c_{44}/\rho)^{1/2}$.

The L modes are responsible for backward stimulated Brillouin scattering and the radial and torsional or mixed torsional/radial modes are responsible for forward Brillouin scattering (Guided Acoustic Wave Brillouin scattering). The latter is further divided into polarized and depolarized GAWBS modes due respectively to R_{0q} and TR_{2q} respectively.

MODE LINEWIDTHS AND SELECTIVE DAMPING

The intensities and linewidths of the depolarized GAWBS resonance's peaks are affected by fiber diameter variations, bulk attenuation of the acoustic wave in the silica optical fiber, and damping on the fiber surface.

The variation in optical fiber diameter (both core and cladding) along its length causes an increase in the mode linewidth. However, it is more significant that the application of a coating on the bare fiber increases the linewidth significantly. This is the result of mode selective attenuation of the guided acoustic waves. When the silica fiber is surrounded by an isotropic material such as the polymer coating or jacket, the coupling of the acoustic radiation from the silica into this medium essentially depends only on the radial displacement U_r at the fiber surface. Acoustic modes with small U values on the surface are
weakly coupled and thus produce GAWBS resonances with high Q. Hence, the lowest frequency TR_{2q} modes turn out to have the largest U values on the surface of the fiber. The higher order modes, on the other hand, have a smaller, more uniform acoustic coupling with the external medium. It is also observed that different mode orders have selective interaction with the damping surrounding the fiber.

CHEMICAL COMPOSITION ON SBS AND GAWBS LINE SHIFTS

SBS

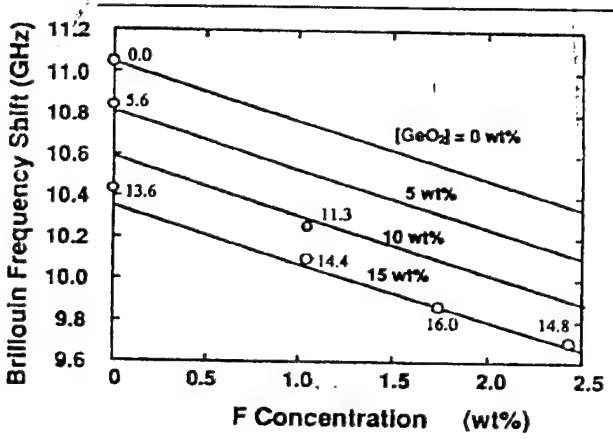

GAWBS

Expected

$$f_m = \frac{V_s y_m}{\pi d}$$

Estimated from Brillouin Shift curves
GAWBS shift ~ 12 Mhz

Observed

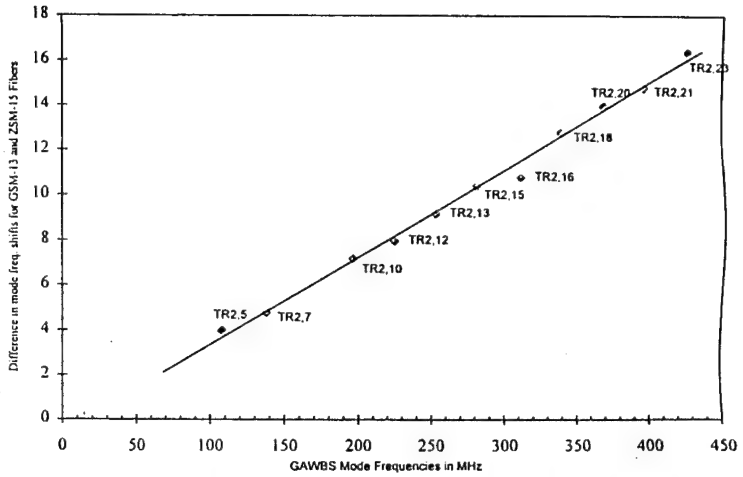

GAWBS Mode Frequency Shifts for *Litespec* GSM-13 and ZSM-15 Fibers

GSM-13: (mole%)

$$\text{core} \begin{cases} G_eO_2 = -2.857 \\ F = -0.091 \end{cases}$$

$$\text{cladding} \begin{cases} G_eO_2 = -0 \\ F = -0.091 \end{cases}$$

ZSM-15:

$$\text{core} \begin{cases} G_eO_2 = -0 \\ F = -0 \end{cases}$$

$$\text{cladding} \begin{cases} G_eO_2 = -0 \\ F = -1.165 \end{cases}$$

TABLE 1
PARAMETERS OF TEST FIBERS FOR BRILLOUIN FREQUENCY SHIFT MEASUREMENT

Fiber	Dopant Concentration of Core		Dopant Concentration of Cladding	Relative Index Difference Δ(%)	Brillouin Frequency Shift* νB (GHz)
	$[GeO_2]$ Δ (%)	[F] Δ (%)	[F] Δ (%)		
A	0	0	−0.35	0.35	11.045
B	0.34	0	0	0.34	10.837
C	0.83	0	0	0.83	10.428
D	0.69	−0.30	−0.30	0.69	10.254
E	0.88	−0.30	−0.30	0.88	10.097
F	0.98	−0.50	−0.50	0.98	9.870
G	0.90	−0.70	−0.70	0.90	9.698

* at 1.55 μm

$$\nu_B = \frac{2n v_L}{\lambda} \qquad \nu_B = 11.045 - 0.277\,[F] + 0.045\,[GeO_2]\ (GHz).$$

DEPENDENCE OF GAWBS BANDWIDTH ON FIBNER CORE SIZE

SBS	GAWBS	
	Expected	Observed

Depolarized GAWBS Modes Bandwidth	Fiber Parameter
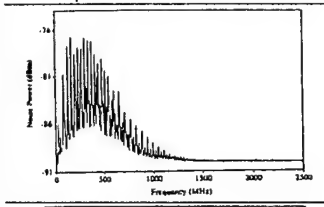	Fiber Length : 900 m Cladding Diameter : 105 μm Core Diameter : 6 μm Δn : 0.0065
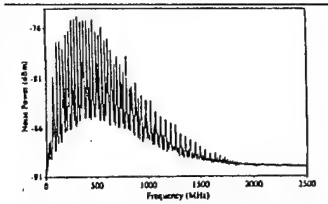	Fiber Length : 1000 m Cladding Diameter : 125 μm Core Diameter : 4 μm Δn : 0.013
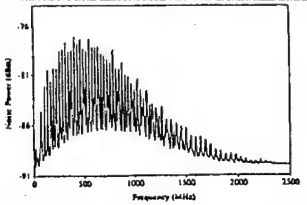	Fiber Length : 200 m Cladding Diameter : 125 μm Core Diameter : 3 μm Δn : 0.025
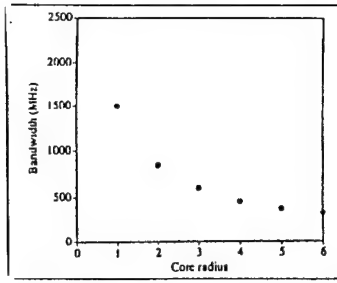	Plot of Depolarized GAWBS bandwidth versus fiber core radius for a fixed fiber diameter of 125 μm.

DEPENDENCE OF GAWBS BANDWIDTH ON FIBER CLADDING SIZE

SBS	GAWBS	
	Expected	Observed

$$\nu_m = \frac{v_d y_m}{2a\pi}$$

$$\therefore \Delta\nu_m / \nu_m = \frac{\Delta a}{a_{mean}}$$

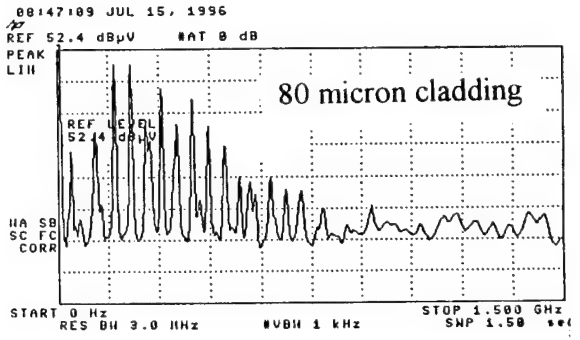

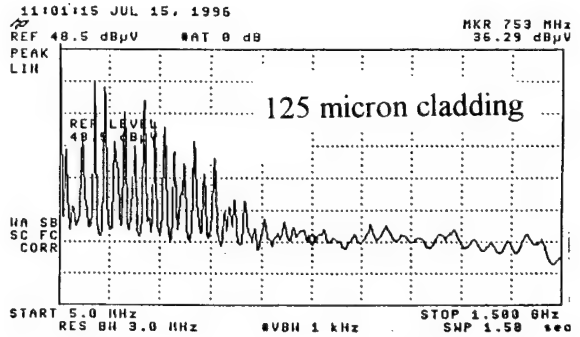

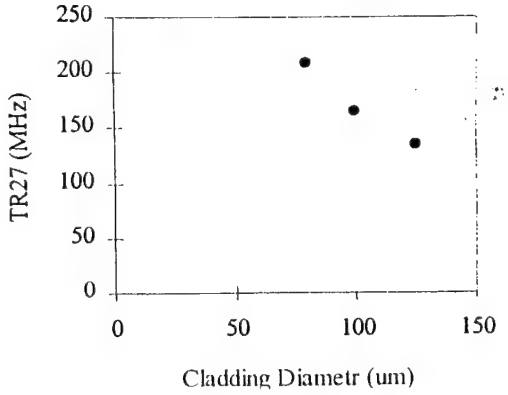

GAWBS LINEWIDTH BROADENING DUE TO COATING

SBS	GAWBS	
	Expected	Observed
		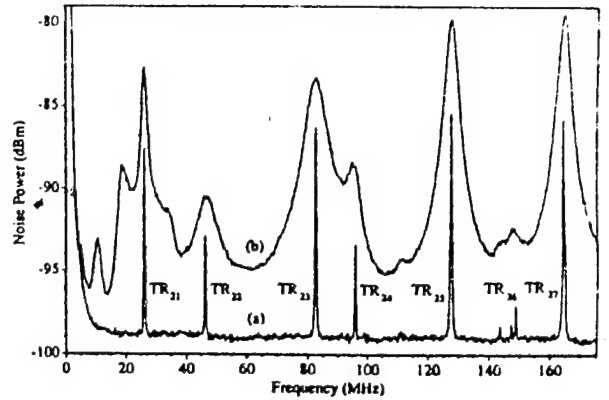
		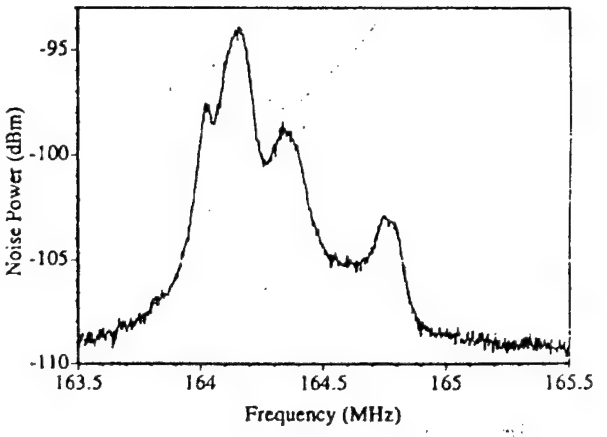

Selective Mode Damping by Fiber Ambient

SBS	GAWBS	
	Expected	Observed

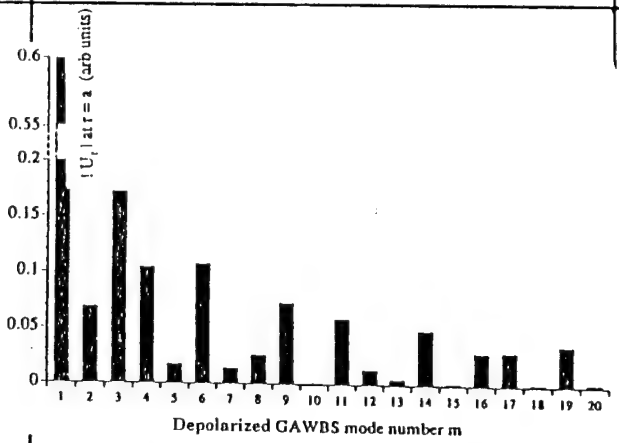

Theoretical calculation of the relative values of U_r at the fiber surface for the depolarized GAWBS modes.

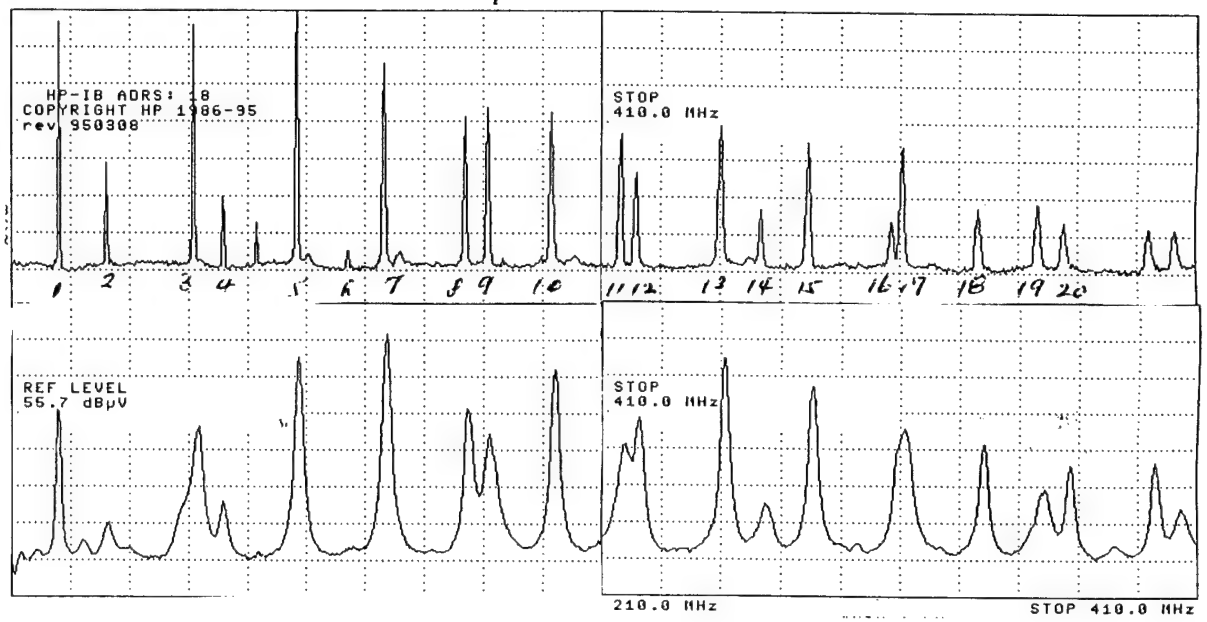

TEMPERATURE EFFECT

SBS	GAWBS	
	Expected	Observed
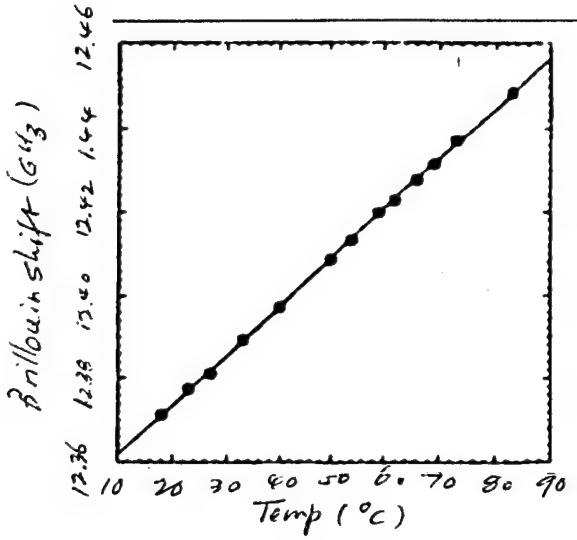	$\Delta(f_B)_\pi \approx 0.10$ GHz = 100 MHz $\Delta(f_B)_\pi / \Delta T \approx$ 100 MHz/80 = 1.25 MHz/°C $\Delta(\delta f_B / \Delta T) = (1/2)\,\Delta(f_{B\pi})\delta\theta$ = 0.5 × 0.08 × 1.25 MHz/°C = 0.05 MHz/°C For T = 100 °C $\Delta(\delta f_B)$ = 5 MHz	

EFFECT OF STRESS/STRAIN IN FIBER

SBS

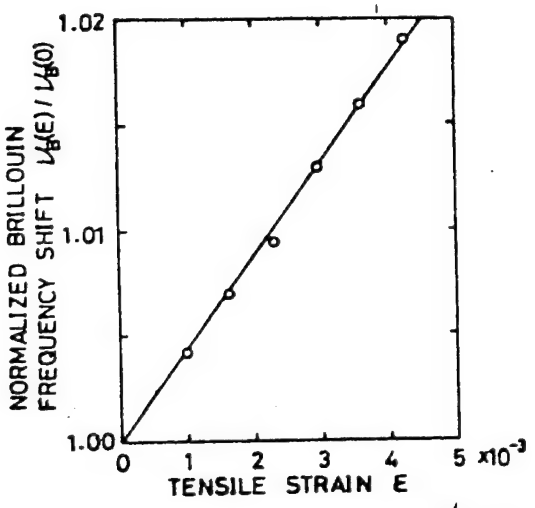

strain Resolution 2×10^{-4}

$\nu_B = 2nV_a/\lambda$

Fiber length 320 m. 2 lasers used

$$V_a = \sqrt{E(1-\kappa)/(1+\kappa)(1-2\kappa)\rho}$$

where E is the Young's modulus, ρ is the fiber density, and κ is the Poisson's ratio.

$(d\nu_B/d\epsilon)/\nu_B = 4.4$. This result shows the potential of Brillouin spectroscopy to evaluate tensile strain in the fiber.

GAWBS

Expected	Observed
$\Delta(f_B)_\pi \approx 0.02 \times 13$ GHz $= 0.26$ GHz $= 260$ MHz $\Delta(\delta f_B) = 0.04 \times 260$ MHz $= 10.4$ MHz	

DISCUSSION ON SENSING

Fiber Parameters, Ambient, SBS and GAWBS

Fiber Parameter	Ambient	SBS			GAWBS				
		Sensing Implication	Frequency Shift	Linewidth	Sensing Implication	Frequency Shift	Spectrum	Bandwidth	Linewidth
Core Doping			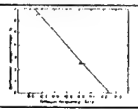	Broad ≈100MHz		Yes	Same		
Cladding Doping					Corrosion	Linear	Same		
Core Diameter								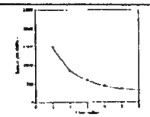	
Cladding Diameter 125μm 100μm 80μm					Mechanical Deformation	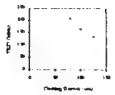			
	Temperature	Yes	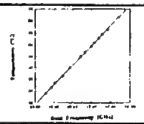		No	No			
	Strain	Yes	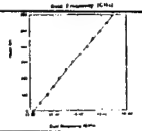		No	No			
	Jacket								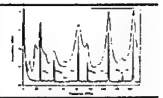
	Index Change								

BIBLIOGRAPHY

Y. Aoki, "Fiber Raman Amplifier Properties for Applications to Long-distance Optical Communications", Opt. And Quantum Electron., Vol. 21, pp. S89, 1989

P. Bayvel and I. P. Gile, "Evaluation of performance parameters of single-mode all-fiber Brillouin ring laser", Optics Letters, Vol. 14, No.11, pp. 581, 1989

A. Corvo and A. Gavrielides, "Forward Stimulated Brillouin Scattering", Applied Physics, Vol.63(11), pp.5220, 1988

D. Cotter, "Transient stimulated Brillouin scattering in long single-mode fiber", Electronic Letters, Vol. 18, No 12, pp. 504, 1982

P. Bayvel and P. M. Radmore, "Solutions of the SBS equations in single mode optical fibers and implications for fiber transmission systems", Electronics Letters, Vol.26, No 7, pp.434, 1990

Y. Hibino and T. Edahiro, "Evaluation of residual stress and viscosity in SiO_2-core/F-SiO_2 clad single-mode optical fibers from Brillouin gain spectra", J. Appl. Phys., Vol. 66, No. 9, pp. 4049, 1989

T. Horiguchi, T. Kurashima, and M. Tateda, "Tensile strain dependence of Brillouin frequency shift in silica optical fiber", IEEE Photon. Tecch. Vol. 1, pp. 107, 1989

N. Shibata, Y. Azuma, T. Horiguchi, and M. Tateda,"Identification of longitudinal acoustic modes guided in the core region of a single-mode optical fiber by Brillouin gain spectra measurements", Opt. Lett. Vol. 13, No. 7, pp. 595, 1988

Jen, J. E. B. Oliveira, N. Goto and K. Abe, "Role of guided acoustic wave properties in single-mode optical fiber design", Elect. Lett., Vol.24, No. 23, pp. 1419, 1988

L. F. Stokes, M. Chodorow and H. J. Shaw, "All-fiber Stimulated Brillouin Ring Laser with Submilliwatt Pump Threshold", Optics Letters, Vol. 7, No. 10, pp. 509, 1982

R. Kadiwar, P. Bayvel and I. P. Giles, "Stimulated Brillouin Scattering in Polarization Maintaining All-fiber Ring Resonators", SPIE, Vol. 985, pp. 338, 1988

P. Bayvel and I. P. Giles and P. M. Radmore, "Transient and Steady-State Characteristics of a Brillouin Amplifier Based on an all-Fiber Single-mode Ring Resonator", Optical and Quantum Electronics, Vol. 21, pp. S113-S128, 1989

E. Desurvire, J. L. Zyslind, and C. R. Giles, "Design Optimization for Efficient Erbium-Doped Fiber Amplifiers", J. Lightwave Technol., Vol. LT-8, No. 11, pp.1730, 1990

E. Desurvire, C. R. Giles and J. R. Simpson, "Gain Saturation Effects in High-Speed, Multichannel Erbium-Doped Fiber Amplifiers at λ=1.53 μm", J. Lightwave Technol., Vol. LT-7, No. 12, pp.2095, 1989

Y. Yamamoto and T. Mukai, "Fundamentals of Optical Amplifiers", Opt. Quant. Electr., Vol. 21, pp. S1-S14, 1989

N. A. Olsson, "Lightwave systems with optical amplifiers", J. Lightwave Technol.,Vol. LT-7, No. 7, pp.1071, 1989

K. Nakagawa, and S. Shimada, "Optical amplifiers in future optical communication systems", IEEE LCS, Vol. 1, No. 4, pp. 57, 1990

R. W. Tkach, A. R. Chraplyvy, and R. M. Derosier, "Performance of a WDM Nettwork Based on Stimulated Brillouin Scattering", Photon. Tech. Lett., Vol. 1, No. 5, pp. 111, 1989

E. Udd, "Fiber optic sensors: An introduction for engineers and scientists", John Wiley & Son, Inc.,1991

R. M. Measures, "Smart Structures with Nerves of Glass", Prog. Aerospace Sci. Vol. 26, pp. 289, 1989

H. S. Hinton, "An Introduction to Photonic Switching Fabrics", New York, Plenum Press, 1993

N. Sttreibl, et al., "Digital Optics",Proceeding of IEEE, Vol. 77, No. 12, 1989

R. Arrathoon, "Optical Computing Digital and Symbolic", New York, Marcel Dekker Inc., 1989

K. Matsushita, et al., "Optical Symbolic Substitution using Lenslet Arrays", Optical Engineering, Vol. 32, No. 4, pp. 847-851, April 1993

P. Fey and K. Brenner, "Computer-Aided Design for Optical Computer Architectures", SPIE, Vol. 1319 Optics in Complex Systems,pp. 179-180, 1990

M. Murdocca, A. Huang, J. Jahns, and N. Streibl, "Optical Design of Programmable Logic Arrays", Applied Optics, Vol. 27, No. 9, pp. 1650-1660, May 1988

W. M. Henry, "Fiber Acoustic Modes and Stimulated Brillouin Scattering", International Journal of Optoelectronics, Vol. 7, No. 4, pp. 453-478, 1992

C. Yu, et al., "Theoretical Considerations of sBs Based All-Optic Switching and Amplification for Computing and Communicatons Applications", The First Annual Symposium on CSA, March 22-23, Graansboro, NC, 1990

R. Kadiwar, P. Bayvel, I. Giles, "Stimulated Brillouin Scattering in Polarization Maintaining All-Fiber Ring Resonators", SPIE Vol. 985 Fiber Optic and Laser Sensors, pp. 338-345, 1988

A. Corvo and A. Gavrielides, "Multiple Short-Pulse Stimulated Brillouin Scattering", Journal of Applied Physics, Vol. 64, No. 2, pp. 489-495, 1988

Stone J., and Chraplyvy A. R. : 'Spontaneous Brillouin noise in long-distance high-bandwidth optical-fiber transmission'. Electronics Letters, Vol. 19, No. 8, 14th April 1983, p. 275-277.

C. K. Jen, and N. Goto, "Backward Collinear Guided-Wave-Acousto-Optic Interactions in Single-Mode Fibers", Journal of Lightwave Technology, Vol. 7, No. 12, pp. 2018-2023, Dec. 1989

D. Marcuse, "Theory of Dielectric Optical Waveguides", Academic Press Inc., 1991

Shelby R. M., Levenson M. D., and Bayer P. W.: 'Guided acoustic-wave Brillouin scattering' . Physical Review B, Vol. 31, No. 8, 15th April 1985, p. 5244-5252.

Shiraki K., and Ohashi M. : 'Sound velocity measurement based on guided acoustic-wave Brillouin scattering'. IEEE Photonics Tech. Lett., Vol. 4, No. 10, Oct. 1992, p. 1177-1180

Ohashi M., Shibata N., and Shiraki K. : 'Fiber diameter estimation based on guided acoustic wave Brillouin scattering'. Optical Fiber Communication Conf., Vol. 5, 1992 OSA Tech. Digest Series, Optical Society of America, Washington DC, 1992, paper WK3.

X. Bao, D. J. Webb, and D. A. Jackson, "Combined Distributed Temperature and Strain Sensor Based On Brillouin Loss in an Optical Fiber", Optics Letters, Vol. 19, No. 2, pp.141-143, 1994

T. Kurashima, T. Horiguchi, and M. Tateda, "Distributed-temperature Sensing Using Stimulated Brillouin Scattering in Optical Silica Fibers", Optics Letters, Vol. 15, No. 18, pp. 1038-1040, 1990

Alistair J. Poustie, "Bandwidth and Mode Intensities od guided acoustic-wave Brillouin scattering in optical fibers", J. Opt. Soc. Am., Vol. 10, No. 4, pp.691, 1993

K. Shiraki, M. Ohashi and M. Tateda, "SBS Threshold of a fiber with Brillouin Frequency Shift Distribution", J. Lightwae Tech., Vol. 14, pp.50, 1996

LIST OF THESES COMPLETED

Name	Degree awarded and year	Thesis Title
Annette Holliday	MSEE, Spring/93	Modeling of Forward Brillouin Scattering in single-mode fiber with applications
Haishan Zhou	MSEE, Fall/92	Feasibility study of fiber ring interferometer applications as low noise sBs oscillator and amplifier
Rodney Scott Shoaf	M.Sc., 1994 (UNCG)	Modal analysis of Guided Acoustic Wave Brillouin Scattering in optical fiber
Reginald Turner	MSEE, May 1995	Experimental implementation of a sBs based MOSD in a fiber ring
Swee Cheng	MSEE, May 1995	Depolarized Guided Acoustic Wave Brillouin Scattering in single mode fibers as resonant forward Brillouin scattering, and its application for sensing
LeMonte Green	MSEE, May 1994	Development of a binary functionally complete optical logic gate utilizing Stimulated Brillouin Scattering in Monomode fiber

LIST OF PUBLICATIONS

C. Yu, and Haishan Zhou, "In Line SBS Based Multi-Channel Near IR Fiber Optic Devices for Amplification, switching and Channel Selection" 15th Intern. Conf. On Infrared and MM Waves, Orland, FL (Dec. 10-14, 1990)

C. Yu, and Annette Holliday, and Haishan Zhou, The Fiber-Brillouin Ring for Low Noise Amplification, Switching and Channel Selection", 23rd Southeastern Symp. On System Theory, Columbia, SC (March 10-12 1991)

C. Yu, and Annette Holliday, "Suppression of Noise in Fiber Amplifier by Fiber Ring", 2nd Annual Symp. On Communications, Signal Processing and ASIC VLSI Design, Greensboro, NC (March 21-22, 1991)

C. Yu, and Haishan Zhou, "Preliminary Studies of the Fiber Ring for Enhancement of SBS Generation in Mid Infrared Fibers", 2nd Annual Symp. On Communications, Signal Processing and ASIC VLSI Design, Greensboro, NC (March 21-22, 1991)

C. Yu, Haishan Zhou, and Swee Cheng, "Optical Fiber Brillouin Noise Amplification for Sensing", Proc. Intern. Conf. Lasers'91, Dec. 9-13, 1991, San Diego, CA

Swee Cheng, Haishan Zhou, and C. Yu, "Fiber Brillouin Ring Laser for Active Inertial Rotation Sensing", Proc. 24th SSST, Greensboro, NC, p. 367

Haishan Zhou, Swee Cheng and C. Yu, "Experimental Investigation of the Optical Noise Sensing Capabilities of the Brillouin Fiber Ring Amplifier", Proc. 24th SSST, March 1-3 1992, Greensboro, NC

C. Yu, Haishan Zhou, and Swee Cheng, "Near and Mid IR Brillouin Active Optical Devices and Applications", Proc. 25th Southeastern Symposium on System Theory, Tuscallosa, Alabama, March 7, 1993

C. Yu, Swee Cheng, Xiaorong Chen, and Scott Shoaf, "GAWBS Based Fiber Vibrational Noise Sensor for Structural Integrity Monitoring', 5th AeroMat Conf. LA, CA, June 6-9 1994

C. Yu, S. Cheng and C. Collier, "Brillouin Active Single Mode Fibers and Sensing", Presented SPIE/95 International Conference, Charleston, SC, December 1995.